Finite Element Analysis of a Controlled Dynamization Device for External Circular Fixation

Análise de elementos finitos de um dispositivo de dinamização controlada para fixação circular externa

Fernando Ferraz Faria[1]   Carlos Eduardo Miers Gruhl[1]   Rafaela Rebonato Ferro[2]
Rodrigo Nunes Rached[3]   Jamil Faissal Soni[4]   Paula Trevilatto[3]

[1] School of Life Sciences, Health Science Department, Pontifícia
Universidade Católica do Paraná (PUCPR), Curitiba, Paraná, Brazil
[2] Orthopedics and Traumatology Department, Hospital Universitário
Cajuru, Pontifícia Universidade Católica do Paraná (PUCPR), Curitiba,
Paraná, Brazil
[3] Graduate Program in Dentistry, School of Life Sciences, Pontifícia
Universidade Católica do Paraná (PUCPR), Curitiba, Paraná, Brazil
[4] Graduate Program in Medicine, Pontifícia Universidade Católica do
Paraná (PUCPR), Curitiba, Paraná, Brazil

Address for correspondence   Paula Trevilatto, PhD, Pontifícia
Universidade Católica do Paraná, Curitiba, PR, Brazil
(e-mail: paulatrevilatto@pucpr.br).

Abstract

Objective   To virtually prototype a device for external circular fixation of long bone fractures with controlled dynamization made of two different materials and predict their mechanical behavior by using the finite element analysis (FEA) method.

Method   A software was used for 3D modeling two metal parts closely attached by a sliding dovetail joint and a high-density silicone damper. Distinctive FEAs were simulated by considering two different materials (stainless steel or titanium), modes (locked or dynamized) and loading conditions (static/point or dynamic/0.5 sec) with uniform 150 kg axial load on top of the device.

Results   The finite elements (FEs) model presented 81,872 nodes and 45,922 elements. Considering stainless steel, the maximum stress peak (140.98 MPa) was reached with the device locked under static loading, while the greatest displacement (2.415×10^{-3} mm) was observed with the device locked and under dynamic loading. Regarding titanium, the device presented the maximum stress peak (141.45 MPa) under static loading and with the device locked, while the greatest displacement (3.975×10^{-3} mm) was found with the device locked and under dynamic loading.

Conclusion   The prototyped device played the role of stress support with acceptable deformation in both locked and dynamized modes and may be fabricated with both stainless steel and titanium.

Keywords
► fractures, bone
► external fixators
► fracture healing
► dynamization

Resumo

Objetivo Construir um protótipo virtual de um dispositivo de fixação circular externa para fraturas em ossos longos com dinamização controlada a partir de dois materiais diferentes e prever seu comportamento mecânico por meio da análise de elementos finitos (AEF).

Método Modelos tridimensionais compostos de duas peças metálicas unidas por uma junta deslizante em rabo de andorinha e um amortecedor de silicone de alta densidade foram criados em um *software*. Análises de elementos finitos distintas foram simuladas considerando dois materiais (aço inoxidável ou titânio), modos (bloqueado ou dinamizado) e condições de carregamento (estático/pontual ou dinâmico/0,5 segundo) diferentes com carga axial uniforme de 150 kg na porção superior do dispositivo.

Resultados O modelo de elementos finitos (EFs) apresentou 81.872 nós e 45.922 elementos. Com aço inoxidável, o pico de tensão máxima (140,98 MPa) foi alcançado com o dispositivo bloqueado e sob carga estática, enquanto o maior deslocamento ($2,415 \times 10^{-3}$ mm) foi obtido com o dispositivo bloqueado e sob carga dinâmica. Com titânio, o pico de tensão máxima (141,45 MPa) ocorreu com o dispositivo bloqueado e sob carga estática, enquanto o maior deslocamento ($3,975 \times 10^{-3}$ mm) foi observado com o dispositivo bloqueado e sob carga dinâmica.

Conclusão O protótipo do dispositivo desempenhou o papel de suporte de tensão com deformação aceitável nos dois modos, bloqueado ou dinamizado, e pode ser fabricado com aço inoxidável ou titânio.

Palavras-chave
► fraturas ósseas
► fixadores externos
► consolidação da fratura
► dinamização

Introduction

The success of biological bone healing seems dependent on a favorable mechanical environment, and, under Wolff's law and Perren's strain theory, several osteosynthesis systems can be used to promote proper stabilization and different types of cell differentiation at the fracture site.[1,2] The relative stability indicated for diaphyseal or comminuted extra-articular fractures allows some controlled mobility at the fracture site and exuberant bone callus formation, which characterizes an indirect or endochondral ossification. To prevent the formation of bulky bone calluses in joint fractures, direct or intramembranous ossification by following absolute fixation with greater stiffness is recommended.[3]

The so-called 'dynamization' refers to the use of external fixation devices to alter the mechanical environment for optimized osteosynthesis. Percutaneous pinning figures as a quick and low-cost method with minimal blood loss, in which external fixators are used to stabilize complex fractures that involve soft tissues or even to progressively correct deformities through stabilization during weight-bearing and mobilization of large joints.[4,5] Moreover, bone callus formation is significantly increased due to the interfragmentary movement, mainly in the optimal range of 0.5 mm for the acceleration of delayed diaphyseal fracture healing.[6] The biocompression theory, which is reported as essential as the osteogenic factors in bone fracture healing, has been proven by finding bone callus in patients with a tibial fracture that were treated with the aid of external fixator to provide good stability and local compression.[7] Accordingly, other authors suggested the use of unilateral external fixators able to promote controlled dynamization in compound fractures and healing delays.[8,9] The use of flexible external fixation to heal long bone fractures has been advocated since 1986 on account of greater mobility and bone callus formation. The first model was employed by Lambotte in 1902, modified by Anderson and Hoffman in 1938, and the classic ring fixator developed by Ilizarov in 1952 remains as a good option due to its versatility, adaptive capacity, low cost, and ability to apply compressive, distractive, or neutral forces on bones.[10–12]

Given the difficulty of conducting clinical investigations on the necessary forces to stimulate bone healing, FEA figures as a useful aid.[13] This method has been widely used in both medical and orthopedic fields since it provides a comprehensive overview of vectors' dissolution in undermined structures, accurate failure detection and still avoids unnecessary costs in cases whereby the failure would only be identified after structural designing or manufacturing.[14] Moreover, the time from the very first conceptual design until production is reduced since the manufacturing of an enormous number of experimental specimens becomes unnecessary. Finite elements analysis provides access to information that is very difficult to obtain in lab conditions, such as the distribution of predicted stress and material strength that are of great importance in the assessment of fatigue resistance.[15,16]
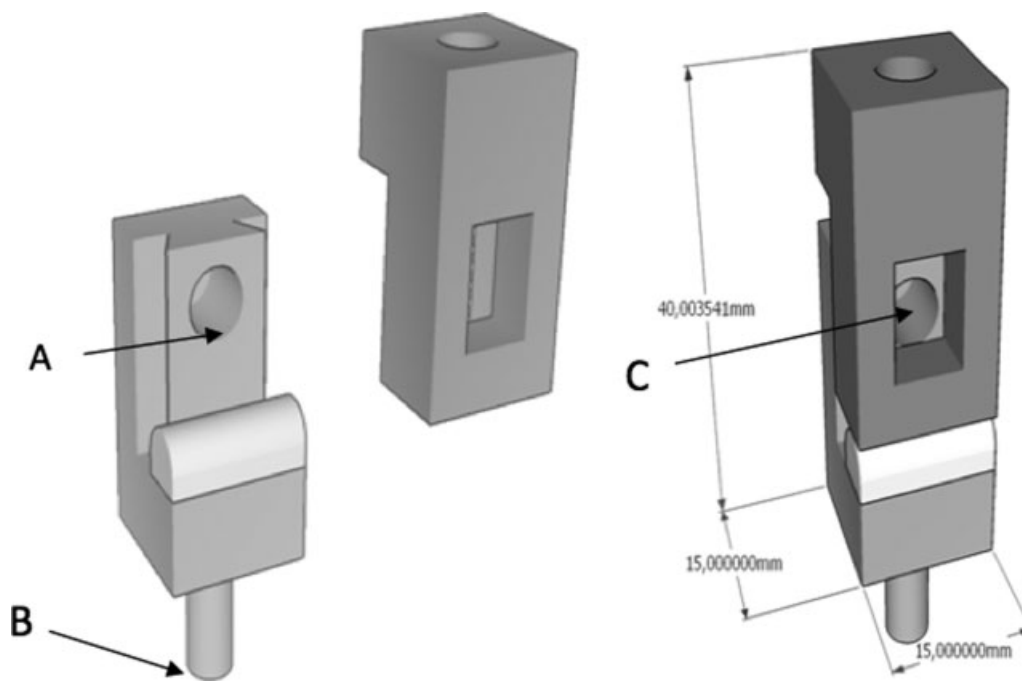
Fig. 1 Geometric modeling. (A) Dovetail slide. (B) Threaded rod. (C) Bolt hole.

Faster consolidation of long bones, better rehabilitation and recovery of the patients are expected due to dynamization, which is still not provided by current external circular fixators. Thus, this study aimed to virtually prototype a device that can connect two rings of standard external circular assembly and promote the dynamization. This prototype was simulated with two different materials, and its mechanical behavior was predicted by using FEA method.

Method

Geometric Modeling

A tridimensional design software (Google SketchUp 2017, Google LLC, Menlo Park, CA, USA) was used to model a device (patent BR 10 2017 018227 4 registered at the National Institute of Industrial Property (INPI, in the Portuguese acronym), consisting of two metal parts closely attached by a sliding dovetail joint and a high-density silicone damper (►**Fig. 1**). The dovetail joint prevents separation of the parts during both torsional and angular movements, while the silicone damper softens and controls axial displacement.

The device was modeled to operate in the locked mode when a single and totally rigid block is formed by screwing both parts together; however, in cases in which dynamization (dynamic mode) is aimed, the physician loosens the bolt to allow sliding movement between the parts and the load is transferred to the bone. A threaded rod is located in the lower part of the device, while the hole observed in the top part allows its versatile attachment to be connected to an external fixator. Moreover, the device has universal applications within different manufacturers due to the standardization of holes, bolts, and rod dimensions.
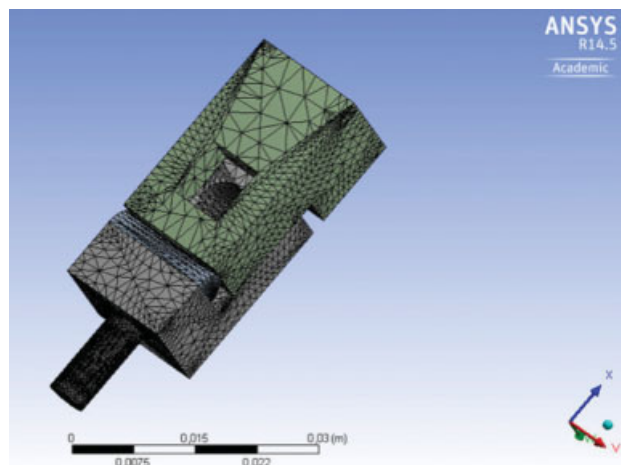
Fig. 2 Finite elements analysis model with 81,872 nodes and 45,922 elements.

Meshing

After geometric modeling, a finite elements (FEs) model was generated by using the Ansys r14.5 software (Ansys Inc., Canonsburg, PA, USA) (►**Fig. 2**). The biomechanical behavior of the device was simulated by considering the physical properties of two different materials indicated by the American Society for Testing and Materials (ASTM) for biomedical applications (stainless steel F138/18Chromium-14Nickel-2.5Molybdenum or titanium F1295/Ti6Al7Nb) in order to predict their feasibility for further machining (►**Table 1**).

Virtual Simulation

By applying a 500 N load, which, in agreement with the FDA (Food and Drug Administration, Department of Health and

Table 1 Physical properties of the materials

Material	Elasticity modulus (MPa)	Poisson ratio	Maximum compression strength (MPa)	Maximum tensile strength (MPa)
Stainless steel	187,500	0.33	800	800
Titanium	113,800	0.34	950	950
Silicone rubber	0.515	0.4	0.0552	0.0552
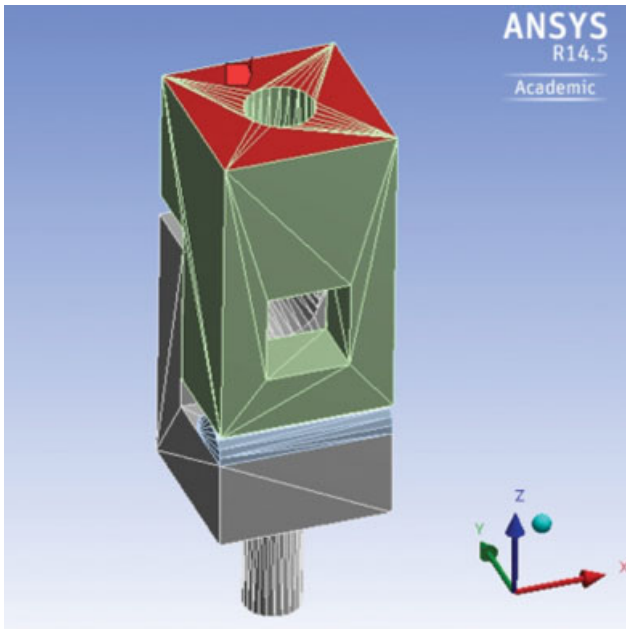
Fig. 3 A 150 kg load was applied to the red area.

Table 2 Results for stainless steel device

Device mode	Locked		Dynamized	
Loading	Static	Dynamic	Static	Dynamic
Maximum stress (MPa)	140.98	80,637	9.2798	9.0956
Maximum displacement (mm)	2.35×10^{-3}	2.41×10^{-3}	2.60×10^{-4}	2.55×10^{-4}

Table 3 Results for titanium device

Device mode	Locked		Dynamized	
Loading	Static	Dynamic	Static	Dynamic
Maximum stress (MPa)	141.45	80.73	9.2015	9.0189
Maximum displacement (mm)	3.86×10^{-3}	3.97×10^{-3}	4.25×10^{-4}	4.17×10^{-4}

Human Services, USA), corresponds to a human body weight of 150 Kg, the model was submitted to the structural analysis of intrinsic displacement, deformation, and fatigue-sensitive site. This load is justified since at least three devices would be simultaneously used in a real-life situation. The load was applied towards the center of the device, on its top surface and with a constant 90° inclination.

In order to simulate both locked (no movement at the fracture site) and dynamic treatment stages (load transfer to the bone and controlled movement are intended), the device was initially tested with both parts completely fixed with one another, and then with the possibility of axial displacement. In both modes, the variables analyzed after loading were the displacement between both device parts and the deformation sites.

The translation resultant between the parts was calculated after applying axial forces with 2 mm as the threshold for acceptable displacement. The deformation thresholds upon axial forces were considered 1 mm for the locked mode and between 1 to 2 mm of compression for the dynamic mode, with re-establishment of the original shape after unloading.[17]

Considering both materials of construction and modes, two distinctive FE analyses were conducted for static (point loading) or dynamic loading (0.5 sec) with uniform 150 kg axial load on top of the device, in order to simulate move-ment or orthostatic standing, respectively (►**Fig. 3**). The device material (stainless steel or titanium), mode (locked or dynamized), and loading condition (static or dynamic) were addressed as independent variables, while resistance and displacement of components were examined as dependent variables.

Results

In compliance with the sequential development of geometric modeling, meshing, constitutive modeling, boundary conditions and loading conditions, our FE model presented a total of 81,872 nodes and 45,922 elements. The FEA results regarding maximum stress and displacement obtained for each material, mode, and loading condition are described in ►**Tables 2** and **3**, while stress distributions are visualized in ►**Figure 4**.

In the simulation with stainless steel, the maximum stress did not reach one-third of the reported mechanical property, which represents reliability against fatigue failure when the locked device is submitted to maximum static loading (maximum stress peak of 140.98 MPa at the proximal area of the dovetail slot); lower values were found for the other simulations, and the lowest stress peak of 9.0956 MPa was observed for the dynamized device under dynamic loading.
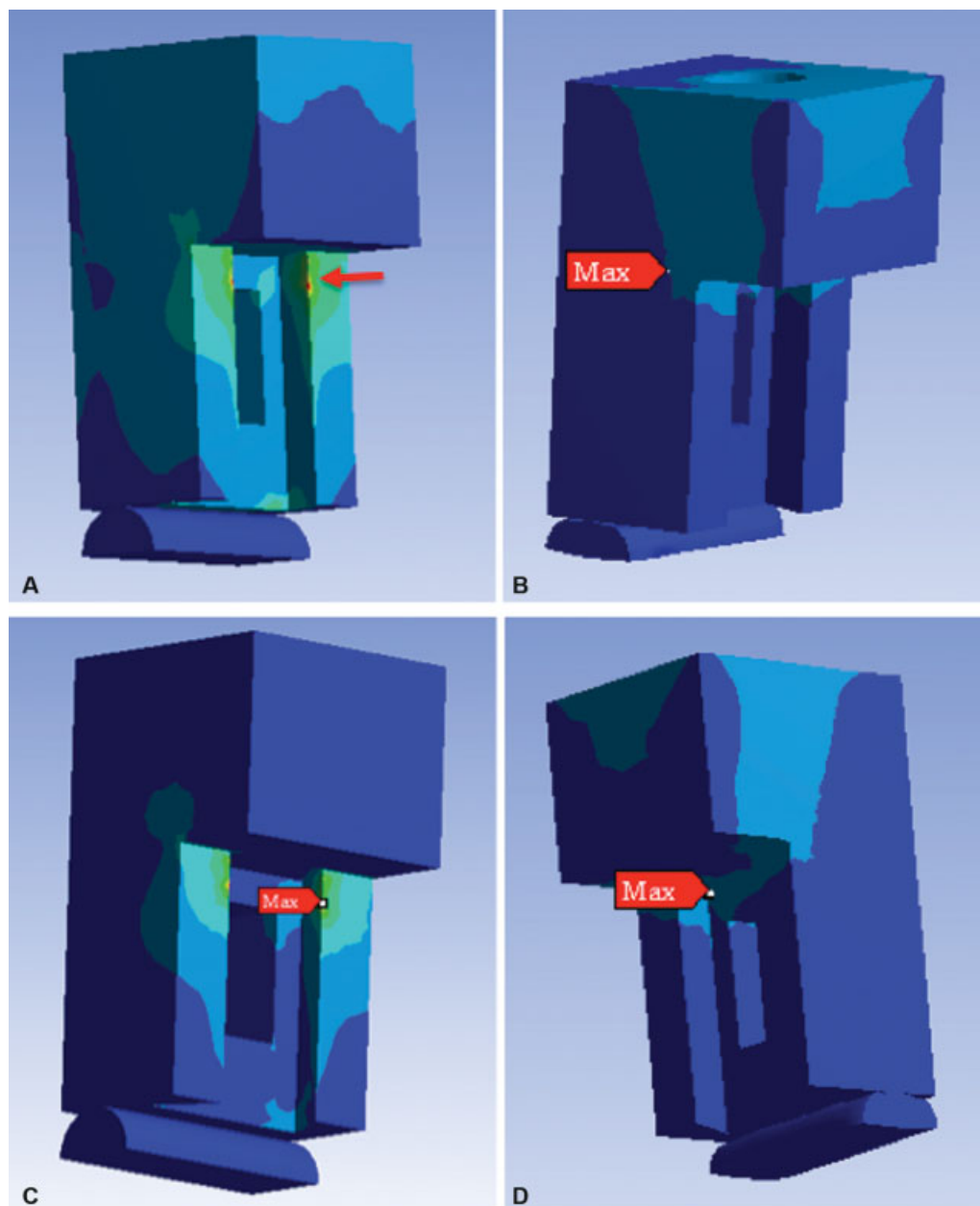
Fig. 4 Finite elements analysis of stress distribution under dynamic loading of the (A) stainless steel device locked, (B) stainless steel device dynamized, (C) titanium device locked and (D) titanium device dynamized. One part of the device was intentionally removed from the image to allow the visualization of the sites of maximum stress peaks (indicated by the red arrows).

In addition, the greatest displacement for the stainless steel device was observed under dynamic loading and with the device locked $(2.415 \times 10^{-3}$ mm); however, this value remained well below the pre-established 1-mm threshold. Displacement was even smaller when dynamization was activated, and the lowest value was observed for static loading $(2.60 \times 10^{-4}$ mm) with a uniform displacement of the dovetail slide; the reliability in promoting controlled axial displacement without interference from device deformation ranged from 1.3477 to 2.3562 safety margin.

Considering titanium as the material of construction, the observed maximum stress was 6.7 times lower than the material property threshold; the highest value (141.45 MPa)

was found for the locked device under static loading (maximum stress peak located at the proximal area of the dovetail slot), and the lowest value was observed for the dynamized device under dynamic loading (9.0189 MPa). The locked device under dynamic loading resulted in the greatest displacement $(3.975 \times 10^{-3}$ mm) at the proximal area of the dovetail slot with a 10.9 safety margin, while the dynamized device under static loading resulted in the lowest displacement $(4.256 \times 10^{-4}$ mm), and the maximum stress peak was located at the proximal area of the dovetail slot. Considering that these values were below the pre-established 1-mm threshold, the effectiveness of the device in supporting axial loading without interference from deformation or mobility was demonstrated.

Discussion

The present study aimed at developing an effective, more accessible, and low-cost device for controlled dynamization to improve the use of a widely known external circular fixator, similar to that introduced by Ilizarov.[10] The device for external circular fixation was simulated with materials of different physical properties widely used for osteosynthesis: highly rigid stainless steel and titanium with high tensile and compressive strengths.[18]

Concerning different loading during movement or orthostatic standing, our findings reinforced the reliability of the prototyped device on the control of compression and axial displacement. The simulations with stainless steel consistently resulted in higher maximum displacement than titanium; however, these values were always well below the pre-established threshold, thus ensuring effectiveness and safety for realistic axial loading up to 500 N.[19] The analysis of maximum stress varied according to the device dynamization; higher values were found for the locked titanium device in both static and dynamic loading. In contrast, the dynamized stainless steel device showed higher maximum stress in both static and dynamic loading conditions; albeit, these values were lower than one third of the material property.[18] Therefore, both materials of construction were considered equally safe in terms of resistance and overload. In addition to the possibility to be assembled with an external circular fixator without altering its initial functionality, the controlled dynamized device modifies the load distribution for the desired period without needing further surgery.

Although these FEA results support the use of this device for bone fracture healing, our findings must be interpreted with caution, and randomized controlled clinical trials are needed to relate these findings to the clinical function.

Conclusion

It can be concluded that the prototyped device played the role of stress support without deformation in both locked or dynamized modes and may be fabricated with both stainless steel and titanium.

Conflict of Interests
The authors have no conflict of interests to declare.

References

1 Wolff J. Das Gesetz der Transformation der Knochen. Berlin: Hirschwald; 1892
2 Perren S, Boitzy A. Cellular differentiation and bone biomechanics during the consolidation of a fracture. Clin Anat 1978;1:13–28
3 Glatt V, Matthys R. Adjustable stiffness, external fixator for the rat femur osteotomy and segmental bone defect models. J Vis Exp 2014;9(92):e51558
4 Compton J, Fragomen A, Rozbruch SR. Skeletal Repair in Distraction Osteogenesis: Mechanisms and Enhancements. JBJS Rev 2015;3(08):pii: 01874474–201508000–00002
5 Henderson DJ, Rushbrook JL, Stewart TD, Harwood PJ. What Are the Biomechanical Effects of Half-pin and Fine-wire Configurations on Fracture Site Movement in Circular Frames? Clin Orthop Relat Res 2016;474(04):1041–1049
6 Frost HM. Bone "mass" and the "mechanostat": a proposal. Anat Rec 1987;219(01):1–9
7 Lazo-Zbikowski J, Aguilar F, Mozo F, Gonzalez-Buendia R, Lazo JM. Biocompression external fixation. Sliding external osteosynthesis. Clin Orthop Relat Res 1986;(206):169–184
8 Marsh JL, Nepola JV, Wuest TK, Osteen D, Cox K, Oppenheim W. Unilateral external fixation until healing with the dynamic axial fixator for severe open tibial fractures. J Orthop Trauma 1991;5 (03):341–348
9 Barquet A, Massaferro J, Dubra A, Milans C, Castiglioni O. The dynamic ASIF-BM tubular external fixator in the treatment of open fractures of the shaft of the tibia. Injury 1992;23(07): 461–466
10 Foxworthy M, Pringle RM. Dynamization timing and its effect on bone healing when using the Orthofix Dynamic Axial Fixator. Injury 1995;26(02):117–119
11 Moss DP, Tejwani NC. Biomechanics of external fixation: a review of the literature. Bull NYU Hosp Jt Dis 2007;65(04):294–299
12 Fragomen AT, Rozbruch SR. The mechanics of external fixation. HSS J 2007;3(01):13–29
13 Roseiro LM, Neto MA, Amaro A, Leal RP, Samarra MC. External fixator configurations in tibia fractures: 1D optimization and 3D analysis comparison. Comput Methods Programs Biomed 2014; 113(01):360–370
14 Lotti RS, Machado AW, Mazzieiro ET, Landre Júnior J. Scientific application of finite elemento method. Rev Dent Press Ortodon Ortop Facial 2006;11:35–43
15 Easley SK, Pal S, Tomaszewski PR, Petrella AJ, Rullkoetter PJ, Laz PJ. Finite element-based probabilistic analysis tool for orthopaedic applications. Comput Methods Programs Biomed 2007;85(01): 32–40
16 Kluess D, Souffrant R, Mittelmeier W, Wree A, Schmitz KP, Bader R. A convenient approach for finite-element-analyses of orthopaedic implants in bone contact: modeling and experimental validation. Comput Methods Programs Biomed 2009;95(01): 23–30
17 Burgers PT, Van Riel MP, Vogels LM, Stam R, Patka P, Van Lieshout EM. Rigidity of unilateral external fixators–a biomechanical study. Injury 2011;42(12):1449–1454
18 Gao Y, Jin Z, Wang L, Wang M. Finite element analysis of sliding distance and contact mechanics of hip implant under dynamic walking conditions. Proc Inst Mech Eng H 2015;229(06): 469–474
19 Pan M, Chai L, Xue F, Ding L, Tang G, Lv B. Comparisons of external fixator combined with limited internal fixation and open reduction and internal fixation for Sanders type 2 calcaneal fractures: Finite element analysis and clinical outcome. Bone Joint Res 2017; 6(07):433–438